

Influence of Proton Irradiation on the Microstructure and Irradiation-Assisted Stress Corrosion Cracking of 316 Stainless Steel

Yun Soo Lim*, Seong Sik Hwang, Dong Jin Kim, Min Jae Choi
Nuclear Materials Safety Research Division/Korea Atomic Energy Research Institute
1045 Daedeok-daero, Yuseong-gu, Daejeon 305-353, Korea
*Corresponding author: yslim@kaeri.re.kr

1. Introduction

Irradiation-assisted stress corrosion cracking (IASCC) of internal components of a pressurized water reactor (PWR) is considered critical for safe long-term operation. Some cracking of internals made of stainless steel (SS), such as guide tube support pins, baffle former bolts and so on, has been identified [1]. The IASCC mechanism is not fully understood; however, it appears to be closely related to microstructural defects caused by neutron irradiation. Therefore, studies on microstructural changes should be the first step to understand how irradiation defects affect the cracking behavior of these alloys. Proton irradiation is a useful experimental technique to study irradiation-induced phenomena in nuclear core materials instead of neutrons [2]. The objectives of the present work were to investigate the irradiation defects and radiation-induced segregation (RIS) using transmission electron microscopy (TEM) and atom probe tomography (APT) in the proton-irradiated 316 austenitic SS and to discuss their influence on IASCC.

2. Methods and Results

2.1 Material and Proton Irradiation

Type 316 austenitic SS was used in this study. The chemical composition of the alloy is given in Tables 1.

Table 1. Composition of the 316 austenitic SS (wt%)

| Cr | Ni | C | Mo | Mn | Si | Cu | P | Fe |
|------|------|-------|------|------|------|-----|-------|------|
| 16.1 | 10.4 | 0.047 | 2.11 | 1.08 | 0.66 | 0.1 | 0.003 | bal. |

The test alloy was solution annealed at 1100 °C and finally water quenched. Before the proton irradiation, the surfaces of the specimens were mechanically ground and then electrochemically polished in a solution of 50 vol% phosphoric acid + 25 vol% sulfuric acid + 25 vol% glycerol for 15 - 30 s at room temperature. The proton irradiation was performed with the General Ionex Tandatron accelerator at the Michigan Ion Beam Laboratory at the University of Michigan. The irradiation processes were conducted using 2.0 MeV protons at a current range of 40 μA. Details of the irradiation procedure can be found in the literature [3]. The specimens were exposed to four levels of

irradiation of 0.4, 1.6, 2.7, and 4.2 displacements per atom (dpa) at 360 °C. The radiation damage levels in dpa of the samples were calculated with the Stopping and Range of Ions in Matter (SRIM) Version 2008 program using a displacement energy of 40 eV in the 'quick calculation' mode.

2.2 Sample Preparation and Microstructural Analysis

The specimens for optical microscopy and SEM were prepared by chemical etching in a solution of 2 vol% bromine+98 vol% methanol. TEM foils containing the irradiated area were prepared with conventional electro-polishing method. To prepare the TEM specimens, thin foils were mechanically thinned until they were less than 40 μm thick and then electro-jet polished in a 7 vol% perchloric acid + 93 vol% methanol solution at - 40 °C with a current of approximately 80 mA.

The proton-irradiated specimens were investigated using various types of microscopic equipment. The SEM imaging and orientation imaging microscopy by electron back-scattered diffraction were done with the JEOL 5200 (operating voltage 25 kV) and JEOL 6300 (operating voltage 20 kV), respectively. TEM analysis was done with a JEOL JEM-2100F (operating voltage 200 kV) to determine the typical microstructural changes due to proton irradiation.

APT specimens were prepared by a standard approach based on FIB lift-out and annular milling. APT analyses were performed using the CAMECA 4000X HR local electrode atom probe (LEAP) microscope operated in the voltage mode with a specimen temperature of 45 K and an evaporation rate of ~0.005 atom/pulse. Data reconstruction and data analysis were performed using the IVAS 3.6.14 software from CAMECA.

2.3 TEM Results on the Irradiation Defects

The irradiation damages depending on the dpa and the depth of 316 SS were calculated with the Stopping and Range of Ions in Matter (SRIM) 2008 program using a displacement energy of 40 eV in the 'quick calculation' mode. These results are given in Fig. 1. The damage profiles exhibit plateaus roughly up to a depth of 15 μm, as well as subsequent damage peaks near the depth of 20 μm from the irradiated surfaces.

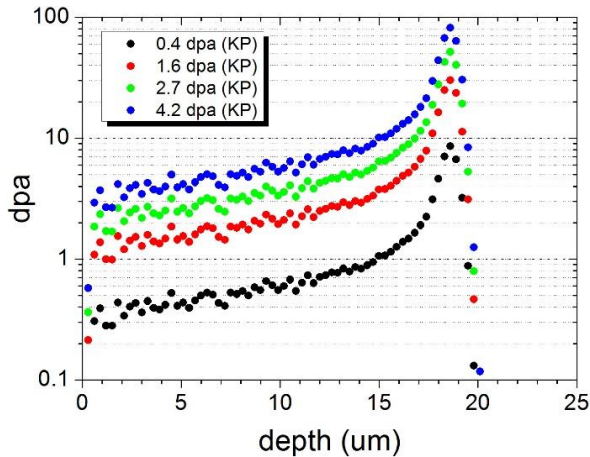


Fig. 1. Calculated dpa-depth profiles of the proton-irradiated 316 SS using the 'quick calculation' mode of SRIM program.

Irradiation of materials with particles that are sufficiently energetic to create atomic displacements can induce a significant microstructural alteration, such as dislocation loops, network dislocations, dislocation channeling, radiation induced precipitation (RIP), voids, cavities, RIS and so on [4]. Fig. 2 shows a bright-field image of Frank loops obtained in the specimen irradiated to 1.6 dpa. In the figure, rod-like shapes resulting from small Frank loops are visible.

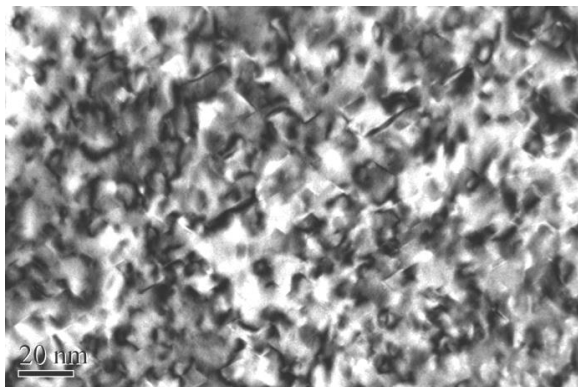


Fig. 2. TEM bright field image showing Frank loops in the 316 SS proton-irradiated to 1.6 dpa.

Fig. 3 is an image showing the micro-voids found in the specimen irradiated to 0.4 dpa. The observation depth of the TEM specimen was approximately 18 μm from the surface. Therefore, the irradiation dose was high at this depth (Fig. 1). The figure was obtained in the under-focus condition, from which the image of the voids could be visualized clearly. The density of the network dislocations also increased considerably by proton irradiation, and the degree of increase seemed to depend on the dose of the proton irradiation. All the present findings are in good agreement with the previously reported results on neutron and proton-irradiated stainless steels.

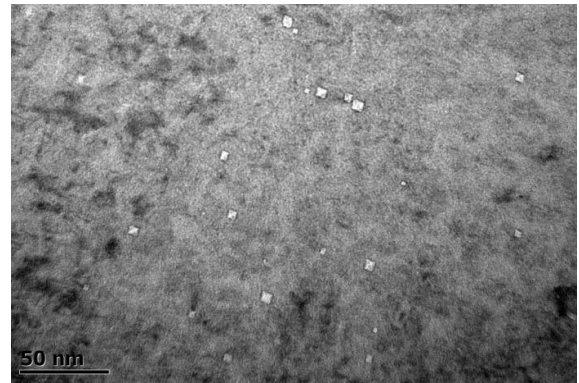


Fig. 3. TEM bright field image showing micro-voids in the 316 SS proton-irradiated to 0.4 dpa.

2.4 APT Results on RIS and Clustering

From the APT analysis of a non-irradiated specimen, it was found that Cr, Si, Mo, C, B and P were lightly enriched at a grain boundary before the proton irradiation. This finding agrees well with the previous result obtained from the solution annealed, non-irradiated austenitic 316 SS [5]. Fig. 4 shows atom maps obtained from the specimen irradiated to 2.7 dpa. The main element Fe did not change significantly at a grain boundary; however, the concentrations of Cr, Mo and Mn decreased at the grain boundary, while Ni, Si, B and P were enriched. The width of the segregated zone for the elements was approximately 10 nm.

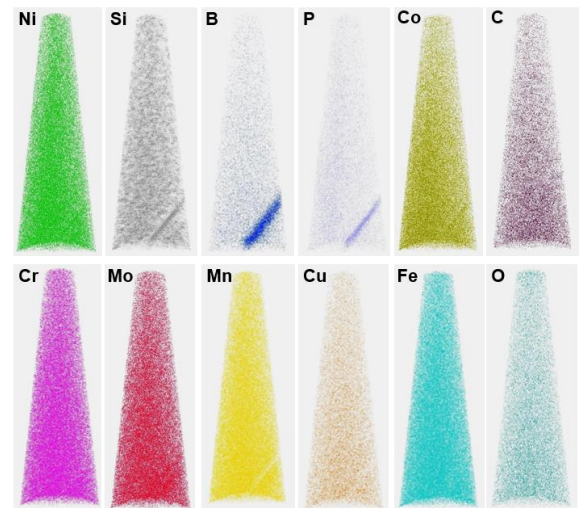


Fig. 4. APT atom maps showing grain boundary segregation in the 316 SS proton-irradiated to 2.7 dpa.

The phenomenon of Cr depletion and Ni and Si enrichment at a grain boundary due to proton or neutron irradiation is well known. From a recent APT observation of irradiated stainless steels [6], it was also identified that Mo and Mn were depleted at a grain boundary.

It is known that Ni and Si elements segregate at grain boundaries and also react with each other to form clusters in the matrix. In the present study, the Ni-Si clusters was also identified in the specimen proton-irradiated to 2.7 dpa. Ni-Si clusters in the matrix have been regularly found in neutron- and proton-irradiated stainless steels, and they are identified as the γ' phase with Ni₃Si composition [7]. It is well known that Ni-Si clusters are the typical radiation-induced precipitates [8].

2.5 Effects of Irradiation on IASCC

The characteristics of microscopic changes by irradiation and their role in changes of material behavior and IASCC have been extensively studied [9]. Irradiation of a material causes hardening, RIS and localized deformation through microstructural and microchemical changes. Radiation-induced hardening basically originates from the introduction of a large amount of small Frank loops (Fig. 2) and network dislocations in the material, which increases the yield stress and lowers the fracture toughness. The increase in the yield strength and the decrease in the fracture stress are large and rapid. Uniform elongation is also reduced sharply when a material is irradiated. As such, the alloy becomes significantly embrittled in the PWR operation condition, which in turn makes it much more susceptible to IASCC by irradiation.

RIS leads to the changes in the grain boundary composition. In the present study, it was found that Cr, Mo and Mn were depleted at the grain boundary, while Ni, Si, B and P were enriched (Fig. 4). It was also reported that Cr depletion at the grain boundaries was closely correlated with component failures [10], which is a phenomenon very similar to that Cr depletion at the grain boundaries in austenitic alloys due to thermal sensitization as the main cause of intergranular cracking. Another factor playing an important role in IASCC is localized deformation. The formation of intense deformation channels that transmit dislocations to the grain boundaries can result in localized slip or sliding of the grain boundary and cause the initiation of intergranular cracks [11]. As a result, the combined effect of hardening, RIS and localized deformation by irradiation can significantly reduce the resistance to IASCC of a structural material under irradiation.

3. Conclusions

Type 316 austenitic SS was irradiated using 2 MeV protons up to 4.2 dpa at 360 °C, and the various irradiation defects were characterized by TEM and APT. Typical irradiation defects mainly consisted of Frank loops, voids and network dislocations. As the dose of the proton irradiation increased, the density of the network dislocations increased. Ni, Si, B and P were enriched, whereas Cr, Mn and Mo were depleted on the grain boundaries associated with RIS. Ni-Si rich clusters,

identified as γ' phase from the previous studies, were also found in the matrix. All the findings were in good agreement with the previous reports.

All of the microstructural and microchemical changes induced by irradiation degrade the mechanical properties of a material. Radiation-induced hardening originating from the introduction of a large amount of small Frank loops and network dislocations in a material causes embrittlement of the material. Cr depletion at the grain boundaries induced by RIS enhances the intergranular cracking of an irradiated material. Therefore, irradiation can significantly reduce the resistance to IASCC of structural components installed near the core region of a PWR.

REFERENCES

- [1] J. McKinley, R. Lott, B. Hall and K. Kalchik, Examination of Baffle-Former Bolts from D.C. Cook Unit 2, Proc. of the 16th Int. Conf. on Environmental Degradation of Materials in Nuclear Power Systems-Water Reactor, 2013.
- [2] J. Gan and G.S. Was, Microstructure Evolution in Austenitic Fe-Cr-Ni Alloys Irradiated with Rotons: Comparison with Neutron-Irradiated Microstructures, Journal of Nuclear Materials, Vol.297, p. 161, 2001.
- [3] G.S. Was, J.T. Busby, T. Allen, E.A. Kenik, A. Jenssen, S.M. Bruemmer, J.Gan, A.D. Edwards, P.M. Scott and P.L. Andresen, Emulation of Neutron Irradiation Effects with Protons: Validation of Principle, Journal of Nuclear Materials, Vol.300, p. 198, 2002.
- [4] A.J. Ardell and P. Bellon, Radiation-Induced Solute Segregation in Metallic Alloys, Current Opinion in Solid State and Materials Science, Vol.20, p. 115, 2016.
- [5] M. Tomozawa, Y. Miyahara and K. Kako, Solute Segregation on Σ 3 and Random Grain Boundaries in Type 316L Stainless Steel, Materials Science & Engineering A, Vol.578, p. 167, 2013.
- [6] K. Fujii and K. Fukuya, Irradiation-Induced Microchemical Changes in Highly Irradiated 316 Stainless Steel, Journal of Nuclear Materials, Vol.469, p. 82, 2016.
- [7] W. Van Renterghem, A. Al Mazouzi and S. Van Dyck, Influence of Post Irradiation Annealing on the Mechanical Properties and Defect Structure of AISI 304 Steel, Journal of Nuclear Materials, Vol.413, p. 95, 2011.
- [8] P.J. Maziasz, Overview of Microstructural Evolution in Neutron-Irradiated Austenitic Stainless Steels, Journal of Nuclear Materials, Vol.205, p. 118, 1993.
- [9] G.S. Was, S.M. Bruemmer, Effects of Irradiation on Intergranular Stress Corrosion Cracking, Journal of Nuclear Materials, Vol.216, p. 326, 1994.
- [10] A.J. Jacobs, G.P. Wozadlo and G.M. Gordon, Low-Temperature Annealing: A Process to Mitigate Irradiation-Assisted Stress Corrosion Cracking, Corrosion, Vol.51, p. 731, 1995.
- [11] M.D. McMurtrey, B. Cui, I. Robertson, D. Farkas and G.S. Was, Mechanism of Dislocation Channel-Induced Irradiation Assisted Stress Corrosion Crack Initiation in Austenitic Stainless Steel, Current Opinion in Solid State and Materials Science, Vol.19, p. 305, 2015.